Assembled Nanodrugs

International Edition: DOI: 10.1002/anie.201509810
German Edition: DOI: 10.1002/ange.201509810

Simple Peptide-Tuned Self-Assembly of Photosensitizers towards Anticancer Photodynamic Therapy

*Kai Liu[+], Ruirui Xing[+], Qianli Zou, Guanghui Ma, Helmuth Möhwald, and Xuehai Yan**

Abstract: *Peptide-tuned self-assembly of functional components offers a strategy towards improved properties and unique functions of materials, but the requirement of many different functions and a lack of understanding of complex structures present a high barrier for applications. Herein, we report a photosensitive drug delivery system for photodynamic therapy (PDT) by a simple dipeptide- or amphiphilic amino-acid-tuned self-assembly of photosensitizers (PSs). The assembled nanodrugs exhibit multiple favorable therapeutic features, including tunable size, high loading efficiency, and on-demand drug release responding to pH, surfactant, and enzyme stimuli, as well as preferable cellular uptake and biodistribution. These features result in greatly enhanced PDT efficacy in vitro and in vivo, leading to almost complete tumor eradication in mice receiving a single drug dose and a single exposure to light.*

Photodynamic therapy (PDT) is a noninvasive treatment of various cancers, and has already been approved for some clinical use.[1] However, photosensitizers (PSs) that are of key importance in PDT have severe limitations, including poor water solubility, poor selectivity towards tumors and low bioavailability.[2] To address these problems, various nanoscale PSs delivery platforms have been developed to improve the bioavailability and tumor targeting, mainly through the enhanced permeation and retention (EPR) effect.[3] However, most of these widely used carriers have relatively complex components (such as synthetic amphiphilic polymers) and largely depend on time-consuming and expensive organic syntheses.[4] Organic solvents and toxic reagents used in chemical synthesis may be incorporated into PSs and lower their biocompatibility.[5] Moreover, nanodelivery systems assembled from amphiphilic polymers inevitably encounter the inherent drawback of relatively low drug loading efficiency ($\approx$10%, w/w),[4a,6] owing to single and weak hydrophobic interaction between drugs and carriers, which fails to overcome the forces responsible for further aggregation or crystallization of drug molecules.[7]

Simple peptides consisting of several amino acids are attractive alternatives to synthetic polymers because of their favorable pharmacological advantages, such as excellent biocompatibility, nonimmunogenicity, high tissue permeability, and rapid clearance from the body.[8] They also have advantages of programmable primary structure, tunable self-assembly architecture and easy availability.[9] However, utilizing such simple components for the design of advanced PSs delivery systems with enhanced PDT efficacy remains a challenge. Thus, it is of great importance to develop strategies based on cooperative interactions and self-assembly of simple peptides and photosensitive drugs.

Herein, we design and prepare nanoscale photosensitive drugs with adjustable functions and responsiveness based on a simple peptide-tuned self-assembly strategy. Amphipathic dipeptides and even amino acids can be used to realize the nanoengineering of PSs based on multiple weak intermolecular interactions, including electrostatic force, π-π stacking, and hydrophobic interactions (Scheme 1). The PSs themselves are considered as one of the building blocks of a drug delivery system with greatly improved PS loading efficiency. The PS loading efficiency is also flexibly tuned based on the stoichiometry between PSs and amphiphilic dipeptides or amino acids. The assembled nanoscale PSs combines many beneficial features in a single delivery platform, including tunable size and composition as well as pH, surfactant, and enzyme-triggered release. Additionally, the weak intermolecular interactions in the assembly make the strategy versatile for various PSs to adapt to specific needs, superior to specialized structures relying on specific binding motifs.

Cationic diphenylalanine (H-Phe-Phe-NH_2·HCl, CDP) derived from diphenylalanine (FF), which is a core recognition motif of the Alzheimer's β-amyloid polypeptide,[10] was used as a model of an amphiphilic dipeptide (Figure S1). 9-Fluorenylmethoxycarbonyl-L-lysine (Fmoc-L-Lys), with a broad spectrum of antiinflammatory activity,[11] was used as a model of an amphiphilic amino acid (Supporting Information, Figure S1). Chlorin e6 (Ce6) was chosen as a model hydrophobic photosensitive drug (Figure S1). An opalescent, cloudy colloidal suspension appeared upon mixing a solution of Ce6 (0.5 mg mL^{-1}) and Fmoc-L-Lys (2.0 mg mL^{-1}) or CDP (2.0 mg mL^{-1}; Figure S2). Scanning electron microscopy (SEM) images of the separated precipitate showed the presence of uniform spherical structures with average diameters of about 100 nm for Fmoc-L-Lys/Ce6 nanoparticles (FCNPs; Figure 1a), and about 200 nm for CDP/Ce6 nanoparticles (CCNPs; Figure 1c) in the given

[*] Dr. K. Liu,[+] Dr. R. Xing,[+] Dr. Q. Zou, Prof. Dr. G. Ma, Prof. Dr. X. Yan
National Key Laboratory of Biochemical Engineering
Institute of Process Engineering
Chinese Academy of Sciences
100190 Beijing (China)
E-mail: yanxh@ipe.ac.cn
Homepage: http://www.yan-assembly.org/
Dr. K. Liu[+]
University of Chinese Academy of Sciences
Beijing 100049 (China)
Dr. Q. Zou, Prof. Dr. H. Möhwald
Max Planck Institute of Colloids and Interfaces
Am Mühlenberg 1, 14476, Potsdam/Golm (Germany)
[+] These authors contributed equally to this work.

Supporting information for this article is available on the WWW under http://dx.doi.org/10.1002/anie.201509810.

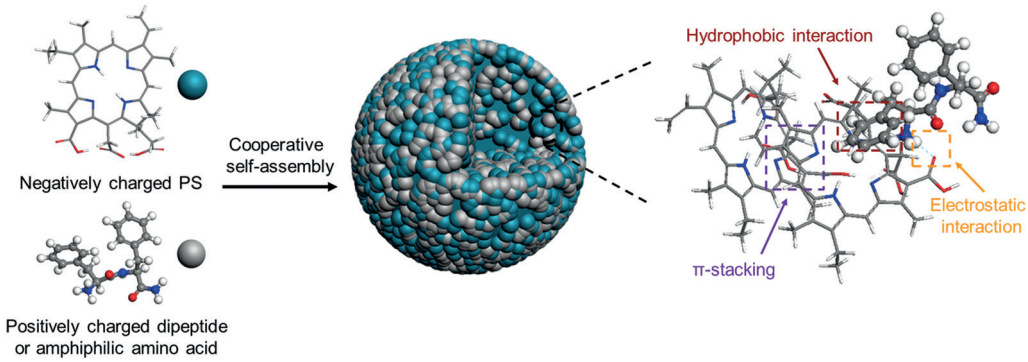

Scheme 1. Fabrication of photosensitive nanoparticles by amphiphilic dipeptide- or amino-acid-tuned self-assembly.

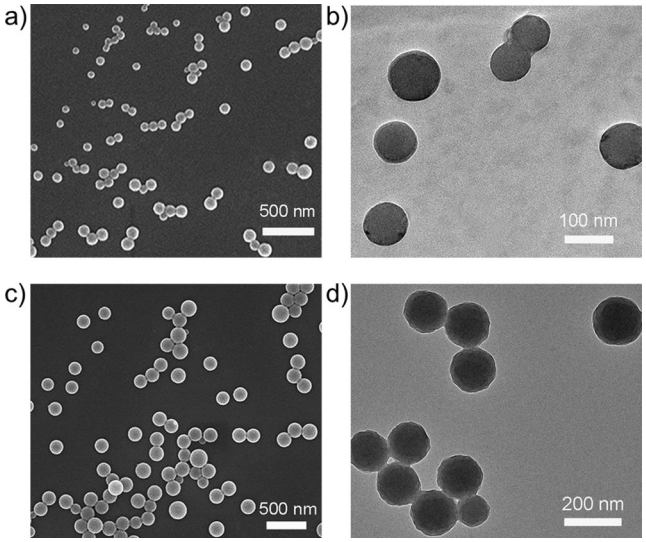

Figure 1. a) SEM and b) TEM image of assembled FCNPs using Fmoc-L-Lys (2.0 mg mL^{-1}) and Ce6 (0.5 mg mL^{-1}) as building blocks. c) SEM and d) TEM image of assembled CCNPs using CDP (2.0 mg mL^{-1}) and Ce6 (0.5 mg mL^{-1}) as building blocks.

stoichiometries. Transmission electron microscopy (TEM) images were characteristic of solid nanospheres (Figure 1b and Figure 1d). Dynamic light scattering (DLS) measurements showed that the hydrodynamic diameter of FCNPs and CCNPs was about 100 nm and 200 nm (Figure S3), respectively, which are close to those derived from SEM and TEM.

The co-assembly of Ce6 with Fmoc-L-Lys or CDP results in a considerably broader and red-shifted Soret band (Figure 2a), as expected for aggregates of different size or structure.[12] The Fmoc groups of Fmoc-L-Lys and the aromatic residues in CDP can interact with the pyrrole groups of Ce6 by hydrophobic and π-π interactions. In a control test, hydrophilic dilysine (KK) was mixed with Ce6, while no NPs were formed (Figure S4). This indicates that hydrophobic and π-π interactions between Fmoc-L-Lys or CDP and Ce6 contribute to the coassembly. The turbidity of the suspension of the NPs decreases in an environment of high ionic strength (Figure 2b), indicating the disassembly of NPs. This suggests the existence of electrostatic forces in the coassembly process. The fluorescence of assembled NPs (such as FCNPs) was dramatically suppressed compared to monomeric Ce6 (Figure S5). The relatively short distance between the Ce6 in the assembly and a significant shift of the Soret band in the absorption spectrum of FCNPs suggest that Dexter-type excitonic migration between Ce6 seems to result in fluorescence quenching.[12,13] Fmoc-L-Lys and CDP possess multiple sites to interact with Ce6. They work as structural defects to reduce the packing efficiency of Ce6, which limits the aggregation to the nanoscale through the synergy of electrostatic, hydrophobic, and π-π interactions.

The particle size and drug loading efficiency can be flexibly tuned by altering the ratio of Ce6 and Fmoc-L-Lys or CDP. For example, as the initial ratio of Ce6 and Fmoc-L-Lys is 1:2, the loading efficiency increases even up to 78% (Table S1), but the particle size is still less than 100 nm (Figure S6). A general strategy to improve the drug loading efficiency is based on the covalent linkage of drugs to carrier materials to form prodrugs.[14] Here, we directly use drugs as

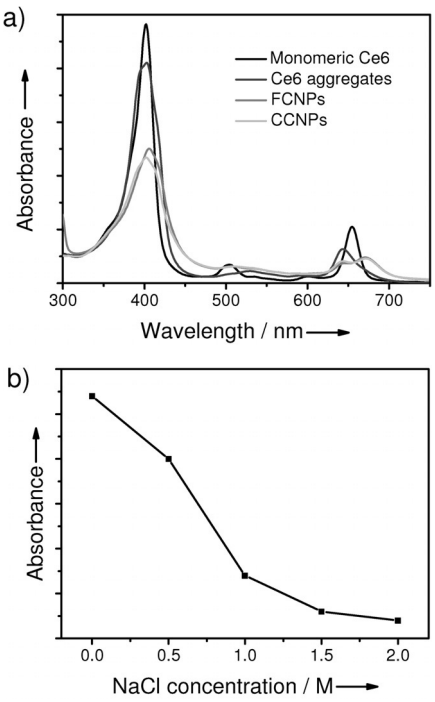

Figure 2. a) UV/Vis absorption spectra of monomeric Ce6 (pH 11.0), individual Ce6 aggregates (pH 6.0), assembled FCNPs (pH 6.0) and CCNPs (pH 6.0). All samples are in water and have the same Ce6 concentration of 0.1 mg mL^{-1}. b) Turbidity of assembled NPs at different salt concentration.

part of a carrier, resulting in a substantially reduced use of carrier material. In addition, the encapsulation efficiency exceeds 80% (Table S1), indicating that this is an efficient strategy for the nanofabrication of hydrophobic PSs. Furthermore, the strategy based on simple peptide-tuned self-assembly is generally suited not only for hydrophobic PSs, but also for water-soluble ones, with formation of well-defined NPs with relatively narrow size distribution (Figure S7 and Figure S8). Significantly, the assembled NPs are stable both in aqueous solution and culture medium (Figure S9), which is suitable for further biological applications.

Taking the greener preparation process of FCNPs into account, we preferentially used it as a model to investigate the responsive release and anticancer PDT efficacy. Owing to the nature of weak intermolecular interactions of the coassembly, the NPs can be responsive to pH, surfactant, and even enzymes, leading to controlled disassembly. The turbidity of the NPs gradually decreases below pH 6.0 (Figure S10), and precipitation finally occurs at pH 5.0, indicating the acid-responsive disruption of the NPs. This may be attributable to protonation of the carboxyl groups of Ce6, weakening the electrostatic forces between Ce6 and Fmoc-L-Lys. Surfactant could also cause the disassembly of the NPs for elimination of hydrophobic interaction between Fmoc-L-Lys and Ce6, as confirmed by the UV/Vis absorption spectrum (Figure S11). It can be envisaged that the hydrophobic domain in endosomes and lysosomes may facilitate the release of Ce6 owing to hydrophobic association. CDP and Fmoc-L-Lys can be responsive to specific enzymes. For example, Fmoc-L-Lys could be hydrolyzed at the amide bond by lipases to generate free Lys at pH 6.0, resulting in disassembly of the FCNPs (Figure S12). Release of assembled NPs in response to low pH, surfactant micelles, and lipases, to some extent mimics the cellular microenvironment, especially that found in lysosomes with pH 5–6, hydrophobic domains, and abundant hydrolases.[15]

The cellular uptake of both FCNPs and CCNPs was evaluated by incubating MCF7 cells with NPs (equivalent Ce6 10 $\mu g\,mL^{-1}$) for 24 h. The red fluorescence (Figure 3a and Figure S13a), corresponding to NPs, emitted from inside the cells, indicating cellular internalization of NPs, presumably by endocytosis.[16] The excellent contrast between the blue nuclear region, green membrane region, and the red cytoplasm (Figure 3a) confirmed that the NPs most likely localize in the cytoplasm. The improved uptake of NPs compared to free Ce6 was confirmed by CLSM observations (Figure S14). In view of the inability of free Ce6 to form large aggregates in the cell medium, nanofabrication of Ce6 by Fmoc-L-Lys- or CDP-tuned self-assembly can apparently improve the cellular uptake. The 3-(4,5-dimethylthiazolyl-2)-2,5-diphenyltetrazolium bromide (MTT) cell survival assay revealed significant anticancer efficacy for both FCNPs and CCNPs compared to free Ce6 under similar conditions (Figure 3b and Figure S13b). According to the IC_{50}, an approximately 4-fold increased photo-cytotoxicity of the NPs, relative to free Ce6, was obtained. No cytotoxicity was observed in the dark (Figure 3b and Figure S14b), further confirming the biocompatibility of the NPs and their potential to destroy tumor cells after light exposure.

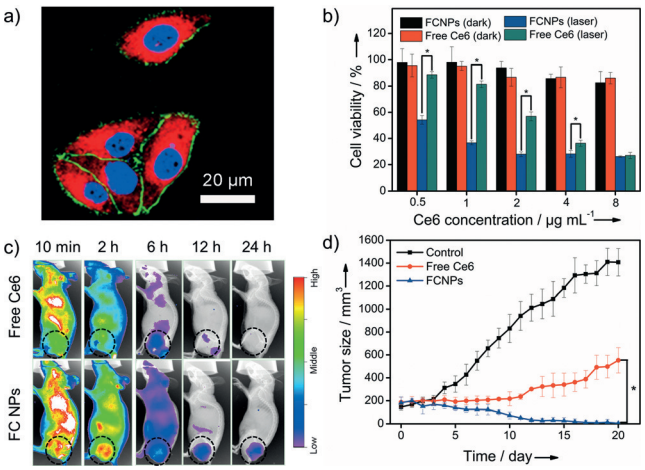

Figure 3. a) Cell internalization of the assembled NPs in vitro. FCNPs (10.0 $\mu g\,mL^{-1}$ of Ce6) were incubated with MCF7 cells for 24 h at 37 °C. Blue nuclei were stained by Hoechst 33342. Green cell membrane is stained by Alexa 488. The red staining is indicative of FCNPs. b) Cytotoxicity of FCNPs and free Ce6 at different Ce6 concentration with or without irradiation ($n=6$). Data represent mean value ± standard deviation. $*p<0.05$ by one-way ANOVA. c) Whole body fluorescence images of MCF7-tumor-bearing nude mice intravenously injected through a tail vein with FCNPs and free Ce6 (equivalent Ce6 4.0 $mg\,kg^{-1}$ body) at different times. Black circles indicate tumor sites. d) Measured tumor growth for 20 days ($n=4$). Data represent mean value ± standard deviation. $*p<0.01$ by one-way ANOVA.

The in vivo biodistribution showed a strong fluorescence signal at the tumor site of both FCNP- and CCNP-treated mice at 2 h post-injection (Figure 3c and Figure S15), indicating selective accumulation of the assembled NPs in the tumor. By contrast, mice treated with free Ce6 showed weaker fluorescence at the tumor site (Figure 3c). In addition, the NPs exhibited sustained Ce6 fluorescence at the tumor site for 24 h, indicating retention of photosensitive drugs in the tumor tissue. The fluorescence intensity observed at 2 h post-injection was higher than that observed at 10 min, and the intensity decreased after 2 h (Figure 3c and Figure S15). An enhanced fluorescence signal at 2 h post-injection may result from disassembly of NPs within tumor sites. As the released Ce6 molecules can be cleared gradually by free diffusion, the fluorescence intensity gets weaker over time. Ex vivo fluorescence images also confirmed the tumor-selective distribution of FCNPs compared to free Ce6 (Figure S16), which may result from the EPR effect.[17] The in vivo therapeutic efficiencies showed that the tumors of FCNP-treated mice were suppressed and almost completely eradicated during the PDT (Figure 3d and Figure S17). However, when treated with free Ce6, the tumor grows back rapidly (Figure 3d and Figure S17). The final tumor volume in FCNP-treated mice is significantly smaller than that for free Ce6 (Figure 3d). This is due to the higher tumor-selectivity of the NPs. No significant body weight variation or organ damage was observed for mice after PDT (Figures S18), preliminarily indicating that the NP-based PDT is a safe anticancer treatment.

In summary, a facile but universal and robust approach to design a photosensitizer delivery system by amphiphilic dipeptide- or amino-acid-tuned self-assembly has been devel-

oped. In this strategy, photosensitive drugs are directly used as building blocks to construct well-defined nanoparticles, resulting in a greatly increased drug-loading efficiency. The assembled nanoparticles have controllable size (20–200 nm) and adjustable loading efficiency (30–80%). The weak intermolecular interactions in the assembled nanoparticles make them responsive to environmental alterations, such as pH, enzymes, and surfactants, similar to the microenvironment in lysosomes of cells. Enhanced anticancer PDT therapeutic efficacy in vivo indicates that the assembled nanoparticles can efficiently deliver photosensitizers to the tumor site by means of the EPR effect and release the photosensitizer. Owing to the flexibility for chemical modification of simple peptides, it can be envisaged that functional peptide sequences can be conjugated to amphiphilic dipeptides or amino acids to enhance drug targeting and control the release of the nanodrugs. Therefore, our developed strategy, based on simple peptide-regulated self-assembly of therapeutic agents into well-defined nanostructures, is suitable for nanodelivery, and provides a non-toxic alternative delivery system for enhanced anticancer therapy.

Acknowledgements

We acknowledge financial support from the National Natural Science Foundation of China (Project Nos. 21522307, 21473208, 91434103, and 51403214), the Talent Fund of the Recruitment Program of Global Youth Experts, the CAS visiting professorships for senior international scientists (Project No. 2015VTA033) and the Chinese Academy of Sciences (CAS) as well as German Max-Planck Society.

Keywords: cooperative self-assembly · nanodrugs · peptides · photodynamic therapy · photosensitizers

How to cite: *Angew. Chem. Int. Ed.* **2016**, *55*, 3036–3039
Angew. Chem. **2016**, *128*, 3088–3091

[1] a) S. B. Brown, E. A. Brown, I. Walker, *Lancet Oncol.* **2004**, *5*, 497–508; b) D. E. Dolmans, D. Fukumura, R. K. Jain, *Nat. Rev. Cancer* **2003**, *3*, 380–387.
[2] D. K. Chatterjee, L. S. Fong, Y. Zhang, *Adv. Drug Delivery Rev.* **2008**, *60*, 1627–1637.
[3] D. Bechet, P. Couleaud, C. Frochot, M.-L. Viriot, F. Guillemin, M. Barberi-Heyob, *Trends Biotechnol.* **2008**, *26*, 612–621.
[4] a) C. F. van Nostrum, *Adv. Drug Delivery Rev.* **2004**, *56*, 9–16; b) G. Pasparakis, T. Manouras, M. Vamvakaki, P. Argitis, *Nat. Commun.* **2014**, *5*, 3623; c) Y. Li, T.-y. Lin, Y. Luo, Q. Liu, W. Xiao, W. Guo, D. Lac, H. Zhang, C. Feng, S. Wachsmann-Hogiu, *Nat. Commun.* **2014**, *5*, 4712; d) W. D. Jang, N. Nishiyama, G. D. Zhang, A. Harada, D. L. Jiang, S. Kawauchi, Y. Morimoto, M. Kikuchi, H. Koyama, T. Aida, *Angew. Chem. Int. Ed.* **2005**, *44*, 419–423; *Angew. Chem.* **2005**, *117*, 423–427; e) S. Y. Park, H. J. Baik, Y. T. Oh, K. T. Oh, Y. S. Youn, E. S. Lee, *Angew. Chem. Int. Ed.* **2011**, *50*, 1644–1647; *Angew. Chem.* **2011**, *123*, 1682–1685.
[5] a) T. M. Allen, P. R. Cullis, *Science* **2004**, *303*, 1818–1822; b) R. Gaspar, R. Duncan, *Adv. Drug Delivery Rev.* **2009**, *61*, 1220–1231; c) K. Liu, Y. Liu, Y. Yao, H. Yuan, S. Wang, Z. Wang, X. Zhang, *Angew. Chem. Int. Ed.* **2013**, *52*, 8285–8289; *Angew. Chem.* **2013**, *125*, 8443–8447.
[6] S. J. Lee, H. Koo, H. Jeong, M. S. Huh, Y. Choi, S. Y. Jeong, Y. Byun, K. Choi, K. Kim, I. C. Kwon, *J. Controlled Release* **2011**, *152*, 21–29.
[7] Y. Zhu, L. Che, H. He, Y. Jia, J. Zhang, X. Li, *J. Controlled Release* **2011**, *152*, 317–324.
[8] a) M. R. Ke, S. L. Yeung, W. P. Fong, D. K. Ng, P. C. Lo, *Chem. Eur. J.* **2012**, *18*, 4225–4233; b) H. Zhang, J. Fei, X. Yan, A. Wang, J. Li, *Adv. Funct. Mater.* **2015**, *25*, 1193–1204; c) Q. Zou, K. Liu, M. Abbas, X. Yan, *Adv. Mater.* **2016**, DOI: 10.1002/adma.201502454; d) R. Ischakov, L. Adler-Abramovich, L. Buzhansky, T. Shekhter, E. Gazit, *Bioorg. Med. Chem.* **2013**, *21*, 3517–3522.
[9] a) C. Chen, K. Liu, J. Li, X. Yan, *Adv. Colloid Interface Sci.* **2015**, *225*, 177–193; b) L. Adler-Abramovich, E. Gazit, *Chem. Soc. Rev.* **2014**, *43*, 6881–6893; c) S. Fleming, R. V. Ulijn, *Chem. Soc. Rev.* **2014**, *43*, 8150–8177; d) Q. Zou, L. Zhang, X. Yan, A. Wang, G. Ma, J. Li, H. Möhwald, S. Mann, *Angew. Chem. Int. Ed.* **2014**, *53*, 2366–2370; *Angew. Chem.* **2014**, *126*, 2398–2402; e) K. Liu, R. Xing, C. Chen, G. Shen, L. Yan, Q. Zou, G. Ma, H. Möhwald, X. Yan, *Angew. Chem. Int. Ed.* **2015**, *54*, 500–505; *Angew. Chem.* **2015**, *127*, 510–515.
[10] M. Reches, E. Gazit, *Science* **2003**, *300*, 625–627.
[11] R. M. Burch, M. Weitzberg, N. Blok, R. Muhlhauser, D. Martin, S. G. Farmer, J. M. Bator, J. R. Connor, M. Green, C. Ko, *Proc. Natl. Acad. Sci. USA* **1991**, *88*, 355–359.
[12] Y. S. Nam, T. Shin, H. Park, A. P. Magyar, K. Choi, G. Fantner, K. A. Nelson, A. M. Belcher, *J. Am. Chem. Soc.* **2010**, *132*, 1462–1463.
[13] G. D. Scholes, *Annu. Rev. Phys. Chem.* **2003**, *54*, 57–87.
[14] K. Cai, X. He, Z. Song, Q. Yin, Y. Zhang, F. M. Uckun, C. Jiang, J. Cheng, *J. Am. Chem. Soc.* **2015**, *137*, 3458–3461.
[15] Y. Urano, D. Asanuma, Y. Hama, Y. Koyama, T. Barrett, M. Kamiya, T. Nagano, T. Watanabe, A. Hasegawa, P. L. Choyke, *Nat. Med.* **2009**, *15*, 104–109.
[16] J. Rejman, V. Oberle, I. Zuhorn, D. Hoekstra, *Biochem. J.* **2004**, *377*, 159–169.
[17] F. Yuan, M. Dellian, D. Fukumura, M. Leunig, D. A. Berk, V. P. Torchilin, R. K. Jain, *Cancer Res.* **1995**, *55*, 3752–3756.

Received: October 25, 2015
Revised: November 10, 2015
Published online: January 25, 2016

